International Journal of Engineering & Technology, 7 (4.19) (2018) 900-908

International Journal of Engineering & Technology

Website: www.sciencepubco.com/index.php/IJET

Research paper

Numerical Investigation of Fluid-Structure Interaction with Mixed Convection in an Open Cavity of Flexible Wall: Effect of Geometrical Parameters

Walaa A. Sabbar*[1], Muneer A. Ismael[2], MujtabaAlmudhaffar[3]

[1, 3]Engineering Technical College, Southern Technical University, Basra, Iraq
[2]Mechanical Engineering Department, Engineering College, University of Basrah, Basrah, Iraq
**Corresponding Author E-mail: walaaadil68@gmail.com*

Abstract

The object of this paper is the mixed convection and fluid flow in a cavity consisting of a flexible wall linked to a horizontal channel. A heat source segment fixed on the bottom wall while all other solid walls are thermally insulated heats up the cavity. Fluid structure interaction (FSI)is taken into account and the arbitrary Lagrangian–Eulerian (ALE) technique with FEM are adopted together to solve the discretized formulations. Impacts of various parameters on the heat exchange were investigated, these are: the channel height to cavity height ratio, represented by (H/D) = 0.5–1.1;heat source length, LH= 0.5 – 1.5;heat source location, and Ri = 0.1- 100. The results show that (H/D) has marginal impact on the Nusselt number, where only 5% enhancement is associated at H/D = 0.7 for Ri = 100. The lower the length of the heat source is the maximal the Nusselt number. A maximum enhancement in the Nusselt number of 156% is obtained when LH is decreased from 1.5 to 0.5.

Keywords: *FSI; open cavity; channel; flexible wall; mixed convection.*

1. Introduction

Although the free convection has been engaged in many industrial situations, mixed free and forced convection plays an important role in lots applications like; solar collectors, emergency-cooling system of nuclear reactors, progressing of metal solidification, and cooling of electronic devices. The interested researcher can see enormous published works regarding the mixed convection in a cavity or enclosures. Amongst these researches, cavity with its upper side is exposed to a continuous flow is found widely in literature. Manca et al. [1], [2] conducted such geometry with constant heat flux as heat source and test edit at different locations. Leong et al. [3] used a channel-open cavity to study the mixed convection heat transfer process. Stiriba [4] performed a numerical treatment in 3-D laminar flow in an open enclosure. Aminossadati and Ghasemi [5] employed a heat source at different locations of a cavity linked with a channel.

Recently, interest has been paid to enhance heat removal to keep the thermal system free of damage due to high temperature represented by using a flexible structure (fin or membrane).This task is implemented by many researcher such as; Al- Amiri and Khanafer [6]; Khanafer [7]; Selimefendigil and Oztop [8]; Selimefendigil and Oztop [9]. Jamesahar et al. [10] used a square cavity partitioned diagonally in to symmetric triangle by flexible thin membrane.

It can be deduced, therefore, that the augmentation of heat transfer in a cavity-channel of rigid walls attracts the interest of many researchers, whereas the role of flexible structure in open cavity has been rarely discussed. Thus, the basic goal of this paper is to focus on the geometrical parameters of the cavity-channel configuration under the interaction between a flexible wall and monitoring the fluid field and heat exchange issues.

2. Theoretical Formulations

The current problem involves an open cavity linked from the topside with a horizontal channel as depicted in Fig. 1. The cavity height and width are D and Lc, respectively. The cavity vertical right wall is set to be flexible while all remainder walls are rigid. The cavity is heated from below by discrete heat source of length LH. The dimensions of the geometry are normalized by *D* and shown in Table 1. The discrete heat source is keptisothermalat higher temperature T_h. Air (Pr = 0.71) enters the channel horizontally from the left side uniformly at u_{in} and cold temperature, T_c. The flow is considered laminar, 2-D and incompressible. The physical properties of the flexible wall and the fluid are considered unchanged with temperature except the density of the fluid which depends on temperature. The flexible wall is considered very thin with high thermal conductivity, and its elasticity modulus (E) does not affected by temperature.

The non-dimensional equations governing the current problem are casted by [12] in vector fasion in the Arbitrary Lagrangian–Eulerian approach (ALE):

For flexible wall;

$$\frac{Ca}{\rho_r}\frac{d^2\mathbf{ds}}{dt^2} - \nabla\boldsymbol{\sigma}=0 \quad (1)$$

$\boldsymbol{\sigma}$ is the stress tensor exertingby the fluid on the elastic wall:

$$\boldsymbol{\sigma} = J^{-1}FSF^T \quad (2)$$

where, $F = (I + \nabla \boldsymbol{d}_s), J = det.(F)$, S is the stress tensor;

$$S = C:(\varepsilon),\ \varepsilon = \frac{1}{2}(\nabla \boldsymbol{d}_s + \nabla \boldsymbol{d}_s^T + \nabla d_s^T \nabla \boldsymbol{d}_s) \quad (3)$$

C is the tensor of elasticity, $C = C(E,v)$,

$$\frac{\partial \theta}{\partial t} = \alpha_r \nabla^2 \theta \quad (4)$$

For fluid field;

$$\frac{\partial u}{\partial t} + \nabla . \boldsymbol{u} = 0 \quad (5)$$

$$\frac{\partial u}{\partial t} + (\boldsymbol{u} - \boldsymbol{w}) \cdot \nabla \boldsymbol{u} = -\nabla \boldsymbol{p} + \frac{1}{Re} \nabla^2 \boldsymbol{u} + Ri * \theta \quad (6)$$

$$\frac{\partial \theta}{\partial t} + (\boldsymbol{u} - \boldsymbol{w}) \cdot \nabla \theta = \frac{1}{Re\, pr} \nabla^2 \theta \quad (7)$$

where $Pr = \frac{\upsilon_f}{\alpha_f}$is the Prandtl number, $Ri = \frac{\beta g (T_h - T_c) D}{u_{in}^2}$is the Richardson number, $Re = \frac{u_{in} D}{\upsilon_f}$is theReynolds's number, Ca=$\frac{\rho_f {u_{in}}^2}{E}$is the Cauchy number, $\alpha_r = \frac{\alpha_f}{\alpha_s}$is the fluid diffusivity to the solid diffusivity ratio, $\rho_r = \frac{\rho_f}{\rho_s}$is the fluid density to the solid density ratio, $\theta = \frac{T - T_c}{T_h - T_c}$is the dimensionless temperature, ν_f is the fluid kinematic viscosity, **u** is the velocity vector of the fluid in dimensional form, **w** is the mesh velocity, *T*is the fluid temperature, ρ_f is the fluid density, β is thermal expansion coefficient.

Mean Nusselt number accounts the convective heat transfer, which is computed by integrating the instant local temperature gradient on the heat source, written as

$$Nu(t)_{avg} = \frac{1}{LH} \int_{LH} \frac{\partial \theta(t)}{\partial y}\, dx \quad (8)$$

LH = is the heat source length.

Dimensionless boundary conditions

1) θ = 1 on heat source segment.

2) θ = 0 (air temperature at channel inlet).

3) u = 1, v = 0 (velocities at the channel inlet).

5) $\frac{\partial \theta}{\partial x}, \frac{\partial \theta}{\partial y} = 0$ (All walls are adiabatic except the inlet and the heat source segment).

6) $\frac{\partial \theta}{\partial x} = \frac{\partial u}{\partial x}$ = v = P= 0 (at outlet of the channel).

7) No slip condition is adopted on the solid boundaries (u = v = 0)

8) The interacting between the fluid and the flexible wall represented by continuities of velocity and stress are governed by two boundary condition as follow:

$$\frac{\partial d_s}{\partial t} = \boldsymbol{u} \quad (9)$$

$$\frac{1}{Ca} \sigma . \boldsymbol{n} = -\boldsymbol{P} + \frac{1}{Re} \nabla \boldsymbol{u} \quad (10)$$

3. Numerical analysis

Owing to the deformable domains, special attention should be focused to interoperate the numerical solution of FSI problems. The literature of numerical solutions implies to an efficient and robust method for this study namely, the ALE method. It interbreeds two numerical procedures namely, the Lagrangian and Eulerian methods. Comprehensive details of this method are illustrated in [13]. In the current study, therefore, this method was used by transforming the governing equations (1),(4) to (7) into the weak format and discretizing them according to the Galerkin finite element [13]. For this task, a COMSOL Multi physics 5.2 was used. This powerful tool has the feasibility of adapting the definition of the equations and the related boundary conditions by dimensionless form. The grid of the present computational domain is conducted using non-uniform triangular grid. A criterion error of 10^{-3} is set to stop the computations. One of the basic requirements of numerical simulation is to check the dependency of numerical solution on mesh size. This step must be carried out before extracting the results. This test was implemented on different values of Nusselt and Richardson numbers for Cauchy and Reynolds numbers of 10^{-4} and 150, respectively. The results are listed in Table 2. By comparing the accuracy and computation time, G3 mesh of 5514 elements is considered as the most suitable compromising between the solution accuracy and its consumed time.

For further validation, a prior problem was resolved, which has been published by Saha and Ali [14] on mixed convection within channel-open cavity of rigid walls heated by a constant heat flux. This validation is performed for Ri = 0.1, Re = 100 and Pr = 0.7. Excellent agreement between the streamlines and isothermal contours were obtained (Fig. 3). Hence, the confirmation of the current numerical solution is trustworthy.

4. Results and Discussion

In this paper, the results were obtained by fixing the following parameters as Prandtl number Pr = 0.71, density ratio ρ_r = 850, Cauchy number Ca = 10^{-4} and Reynolds number Re = 150 and. While the other four parameters are assorted as: Ri = 0.1, 1, 10, and 100,H/D= 0.5, 0.7, 0.9,1 and 1.2, the heater length LH = 0.5, 1 and 1.5 and different heater locations.

To inspect the time at which the thermal field stabilizes, Fig. 4 is established to illustrate the evolution of Nusselt number. For this task, all Richardson number values were inspected. With time, the thermal energy is carried to the fluid and become hotter than the initial state; thus, the temperature disparity becomes lesser. As a result, Nusselt number drops until reaches to steady state condition. Beyond t = 4, the Nusselt number reaches steady state for Ri ≤ 1. While for Ri=10 and100, Nu_{avg} experience some oscillations then settle beyond t = 12 and 8, respectively.

Figure 5 depicts the growth of time of the streamlines and the configuration of the flexible wall. At first, the stress of the fluid flow on the flexible wall is zero. Therefore, the flexible wall shape appears upright while the streamlines are straight and parallel. When time goes on, this behavior changes and the flexible wall arches to the left. A strong vortex is generated inside the entire open cavity and the vortex expands to the outside and obstructs the streamlines in the channel. As well as, a secondary vortex is observed downstream of the cavity. However, beyond t = 12, the streamlines tend to be unchanged, while the elastic wall becomes perfectly stable, with slight curvature to left. Accordingly, the forthcoming results are presented at t = 12.

4.1 The impact of H/D ratio

The channel to cavity ratio (H/D) is changed as 0.5, 0.7, 0.9, 1 and 1.2forRi = 10. Figure 6portrays the streamlines and flexible wall with H/D. At very low H/D = 0.5, the limited channel flow area leads to generate a recirculation occupies the whole cavity which forces the elastic wall to bend outside the cavity due to the restricted flow in the channel. The oscillation of the flexible wall between bending inside the cavity (because the buoyancy effect) and reserving its straight original shape (equivalent inertia and buoyancy forces) is noticed when H/D ≥ 0.7, where the available flow passage is relatively higher. The isotherm lines, presents uniform temperature distribution within the cavity, while the temperature gradient expands to a substantial zone within the channel forming plume-like pattern skewed to the right, which implies to a dominant heat convection.

The influence of (H/D) ratio on $Nu_{avg}$is depicted in Fig. 7. This figure explains thata slight decrease of Nu_{avg} when Richardson number is 0.1 ≥ Ri≥1. Hence, this indicates to adverse impact of the H/D consolidates when the convective streams rise from the cavity. ForRi =10,the highest marked increase in the Nusselt

number is at H/D = 1 which implies to strengthen heat convection of about 8.7% higher than other H/D values. For Ri = 100, the maximum Nusselt number is associated at H/D = 0.7 with 5% greater than other ratios.

4.2 The Impact of the Heater Length

Three values of the heater length are investigated; LH = 0.5, 1 and 1.5 atRi = 10. Figure 8 presents that at the lowest heat source length (LH= 0.5),the flexible wall looks completely vertical, this because the inertia force and buoyancy force are approximately equal. The flexible wall is slightly bent inside the cavity at LH ≥1.The streamlines form a single vortex, which split into two vortices at maximum value of LH. Inside the cavity, the isothermal lines portray a uniform distribution of temperature with steeper gradient near to the heater. This steep gradient develops with increase of LH, which implies to dominant heat convection.
The influence of heat source length on the Nusselt number is illustrated in Fig. 9. The behavior of this figure is widely explained in the literature, namely the Nusselt number proportional inversely with the heater length. This means that the heat transfer decrease when LH increases. For example, When LH is decreased from 1.5 to 0.5, the increase in the Nusselt number are 120% and 156% at Ri = 0.1 and 100, respectively.

4.3 The Effect of the Heat Source Location

Three locations were inspected; the heater is fixed near the rigid left wall, in the mid-span, and close to the flexible wall and following the terms (SL, SM and SR), respectively. The impact of these three patterns on the flow, thermal field, and the flexible wall shape for Ri = 10 is depicted in Figure 10.The flexible wall manifested approximately vertical attitude because the equivalent effect of the inertia and bouncy force. The isothermal lines possess a regular temperature distribution within the cavity as illustrated in SL and SM. While in SR, the convective rising fluid nearby the flexible wall forces the flexible wall and pushes it to the right. The isotherms experience distinguished gradients close to the flexible wall and steeper temperature gradient nearby the heater, which refer to the powerful convection.
Fig. 11portrays the Nusselt number with Richardson number. It can be inferred that Nu_{avg} of SM location is markedly higher than the other patterns, where an increase in Nusselt number about 57% is recorded at Ri = 1. The enhancement of the Nusselt number of SM location increases rapidly with Ri due to development of the natural convection which included the entire cavity. When Ri≥ 10, the enhancement of the Nusselt number of SR location becomes faster than SL location. This because in SR position, the contribution of the wall flexibility features with the convective fluid becomes more announced.

5. Conclusions

Combined convection in a flexible wall cavity-channel domain is studied numerically. In this study, the attention has been focused on the geometrical aspects of the problem. The Galerkin finite element approach implemented with ALE procedure is followed. The following remarks have been drawn from this study.

- Nusselt number drops with time until reaches to steady state condition. Beyond t = 4, Nu_{avg} reaches to steady state for Ri = 0.1 and 1. For Ri=10 and 100, Nu_{avg} oscillates then stabilizes beyond t = 12 and 8, respectively**.**
- The ratio of the channel and the cavity heights(H/D) has a slightly influence on the rate of heat exchange, the average Nusselt number increases as H/D decrease from 0.5 to 1.2.
- The best augmentation of heat transfer rate is obtained at minimum length of the heater. For example, when the heater length is decreased from 1.5 to 0.5, the increase in the Nusselt number are 120% and 156% at Ri = 0.1 and 100, respectively.
- The better position of the heater is in the mid span of the cavity bottom wall compared to other locations, where an increase in Nusselt number about 57% is recorded with this location at Ri = 1.

Considering non-Newtonian fluid is one of the future works of the present investigation.

References

[1] O. Manca, S. Nardini, K. Khanafer, K. Vafai, Effect of heated wall position on mixed convection in a channel with an open cavity, Numerical Heat Transfer: Part A: Applications 43(2003)259–82.
[2] O. Manca, S. Nardini,R. Pitzolu,K. Vafai, Experimental investigation on mixed convection in a channel with an open cavity, ASME Summer Heat Transfer Conference (2003) 257–267.doi:10.1115/HT2003-47132.
[3] J.C. Leong,N.M. Brown,F.C. Lai, Mixed convection from an open cavity in a horizontal channel, Int. Commun Heat Mass Transfer 32(2005)583–92.
[4] Y. Stiriba, Analysis of the flow and heat transfer characteristics for assistingincompressible laminar flow past an open cavity,IntCommun Heat Mass Transfer 35 (2008)901–907.
[5] S.M. Aminossadati, B. Ghasemi, A numerical study of mixed convection in a horizontal channel with a discrete heat source in an open cavity. European Journal of Mechanics-B/Fluids 28 (2009)590–598.
[6] A. Al-Amiri, K. Khanafer, Fluid–structure interaction analysis of mixed convection heat transfer in a lid-driven cavity with a flexible bottom wall. Int J Heat Mass Transfer 54 (2011) 3826–3836
[7] K. Khanafer, Comparison of flow and heat transfer characteristics in a lid-driven cavity between flexible and modified geometry of a heated bottom wall. Int J Heat Mass Transfer 78 (2014)1032–1041 .
[8] F. Selimefendigil, H.F. Öztop, Analysis of MHD mixed convection in a flexible walled andnanofluids filled lid-driven cavity with volumetric heat generation. Int J MechSci118 (2016)113–124.
[9] F. Selimefendigil, H.F. Öztop, Natural convection in a flexible sided triangular cavity withinternal heat generation under the effect of inclined magnetic field. J MMM 417 (2016) 327–337
[10] E. Jamesahar, M. Ghalambaz, A.J. Chamkha, Fluid-solid interaction in natural convection heat transfer in a square cavity with a perfectly thermal conductive flexible diagonal partition. Int J Heat Mass Transfer 100 (2016)303–319.
[11] S.A.m. Mehryan, A.J. Chamkha, M.A. Ismael, M. Ghalambaz, Fluid–structure interaction analysis of free convection in an inclined square cavity partitioned by a flexible impermeable membrane with sinusoidal temperature heating. Meccanica52 (2017)2685–2073.
[12] M. Ghalambaz, E. Jamesahar, M.A. Ismael, A.J. Chamkha , Fluid-structure interaction study of natural convection heat transfer over a flexible oscillating fin in a square cavity. Int J ThermSci111 (2017)256–273.
[13] J. Donea, A. Huerta, Finite element methods for flow problems, John Wiley Sons, 2003
[14] S. Saha, M. Ali, Finite Element Analysis of Mixed Convection in an Open Cavity Heated from Below.Proceedings of the International Conference on Fluid and Thermal Energy Conversion111 (2006) 1–9.

Nomenclatures

Ca Cauchy number, $Ca = \rho_f u_{in}^2 / E$
ds displacement vector (m)
D cavity height (m)
E Elasticity modulus of the flexible wall (N m^{-2})
Fv body force vector in the flexible wall (N m^{-3})
g acceleration (m s^{-2})

H channel height (m)
k thermal conductivity ($Wm^{-1}K^{-1}$)
n normal vector
Nu Nusselt number
P pressure ($N\ m^{-2}$)
Pr Prandtl number, $Pr = \nu_f / \alpha_f$
Re Reynolds number, $Re = u_{in} D/\nu_f$
Ri Richardson number, $Ri = g\beta(Th - Tc)D/u_{in}^2$
t dimensionless time
T temperature (K)
x,y Cartesian coordinates
u velocity vector ($m\ s^{-1}$)
wmesh velocity ($m\ s^{-1}$)

Greek symbols

αthermal diffusivity ($m^2\ s^{-1}$)
β volumetric thermal expansion coefficient (K^{-1})
νkinematic viscosity ($m^2 s$)
ρ density ($kg\ m^{-3}$)
θ dimensionless temperature

Subscripts

avg average
c cold
f fluid
h hot
in inlet
r ratio
s solid

Table 2: Dimensions of the problem under steady with respect of D

H/D	Li/D	Le/D	LH/D	Lc	L
0.5 – 1.1	1	2	0.5	2	0.75

Table 2: Grid independencetestofNu_{avg}atRe =150,Ca=10^{-4}, Pr=0.71

Ri	G1 (2681)	%Error	G2 (3618)	%Error	G3 (5514)	%Error	G4 (13572)	%Error
0.1	5.207	-	5.336	2.5	5.378	0.8	5.614	0.8
1	7.339	-	7.477	1.9	7.476	0.01	7.539	8.4
10	12.58	-	12.72	1.1	12.267	-3.5	12.832	4.6
100	19.484	-	20.002	0.15	20.224	1.1	20.392	0.83

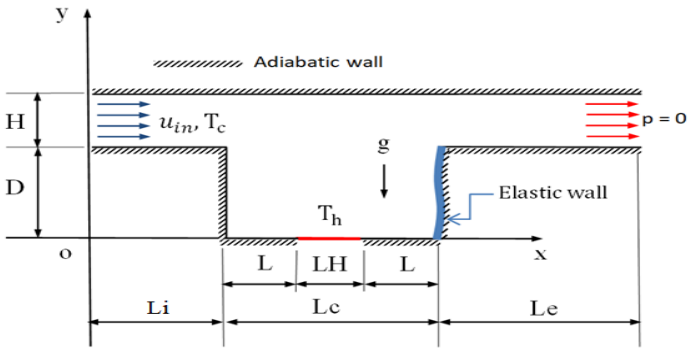

Fig. 1: Schematic of problem description

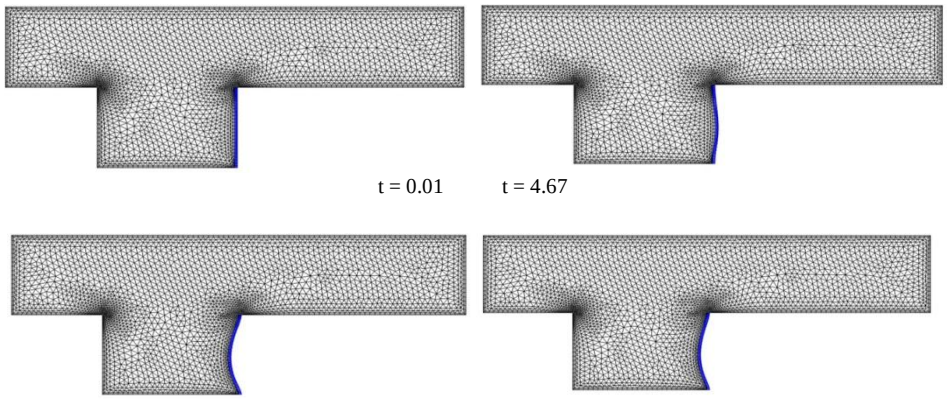

Fig. 2: variation of mesh deformation with time for Ri = 100, Re = 150, H/D = 1 and Ca = 10^{-4}.

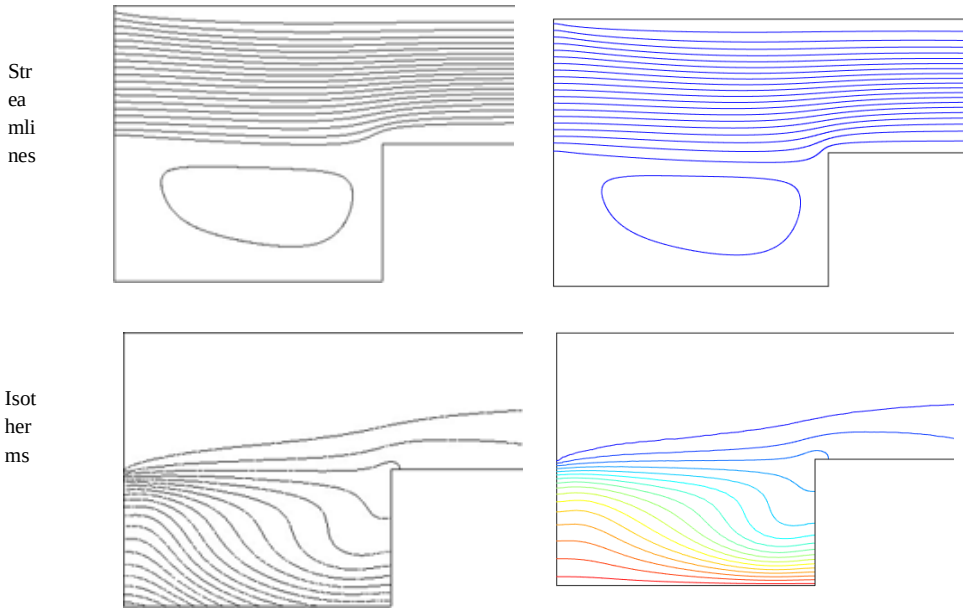

Fig. 3: Comparison of contour maps with Saha and Ali for Re = 100, H/D = 1, Richardson number Ri =0.1.

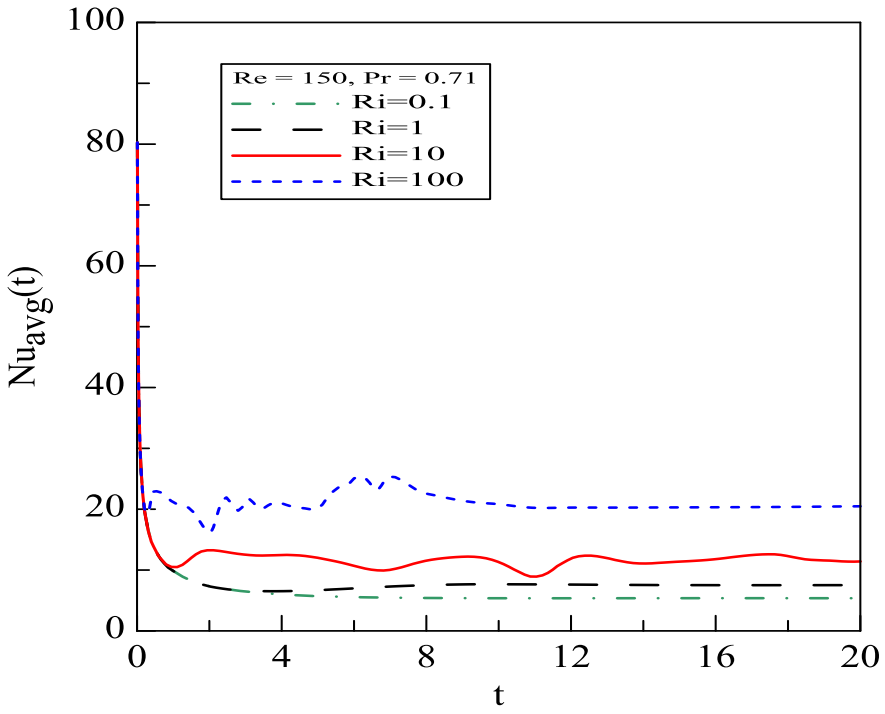

Fig. 4: Evolution of Nu_{avg}withRichardsonvalues at Ca =10^{-4} and Re = 150.

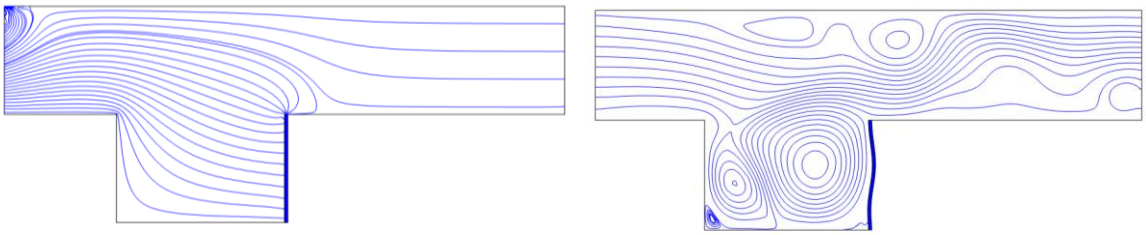

(t) = 0.01 (t) = 4

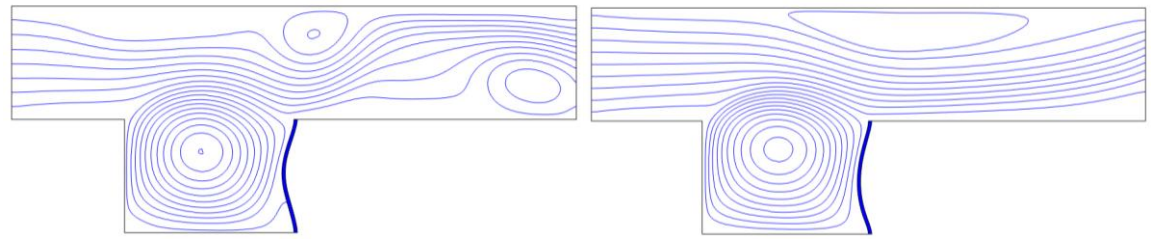

(t) = 8 (t) = 12

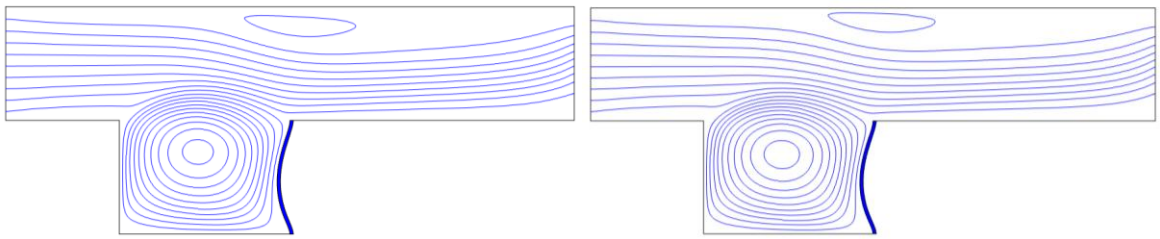

(t) = 16 (t) = 20

Fig. 5: Streamlines and configuration of the flexible wall against time for Re = 150, Ca = 10^{-4} and Ri = 10.

Streamlines Isotherms

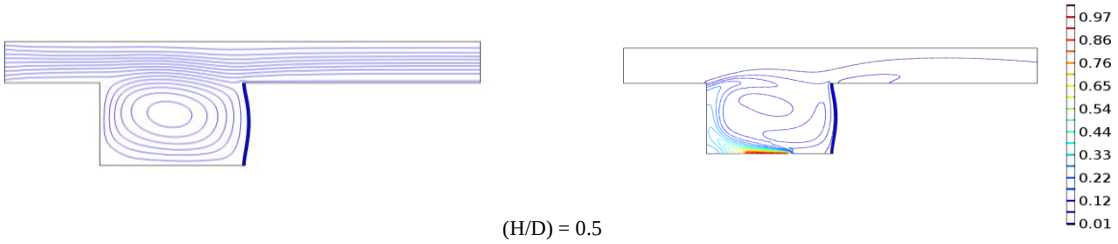

(H/D) = 0.5

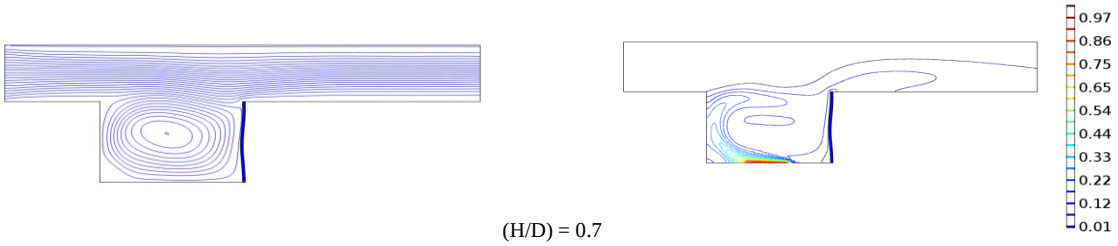

(H/D) = 0.7

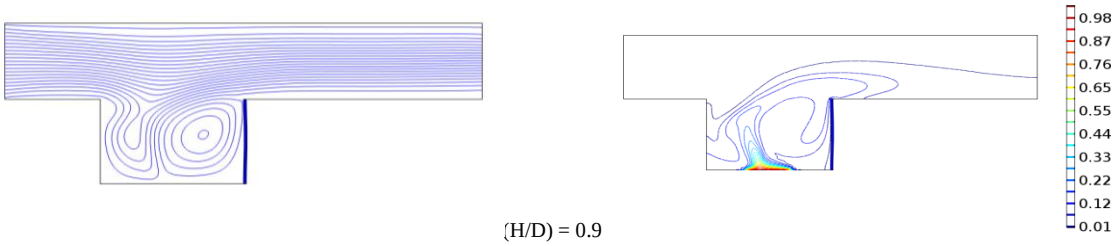

(H/D) = 0.9

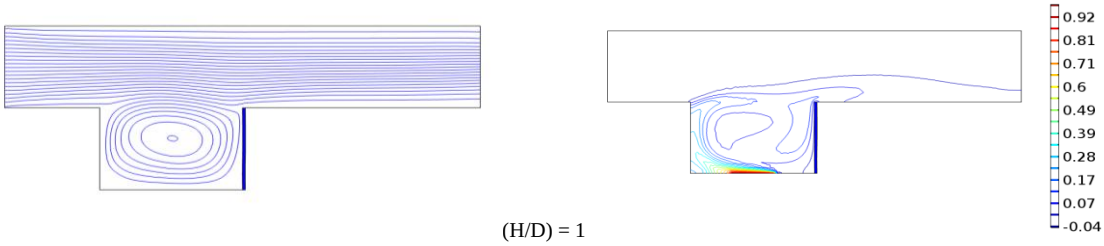

(H/D) = 1

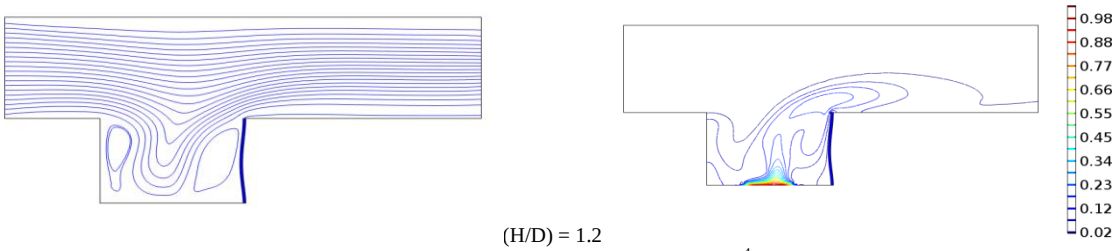

(H/D) = 1.2

Fig. 6 Contour maps for different values of (H/D) when Ca = 10^{-4}, Ri = 10, Re = 150

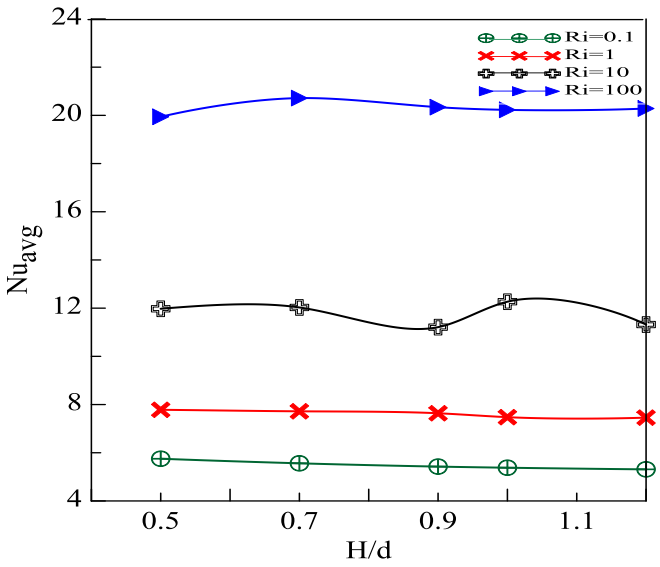

Fig. 7: Mean Nusselt number with H/Dat Re = 150 and Ca = 10^{-4}.

Streamlines Isotherms

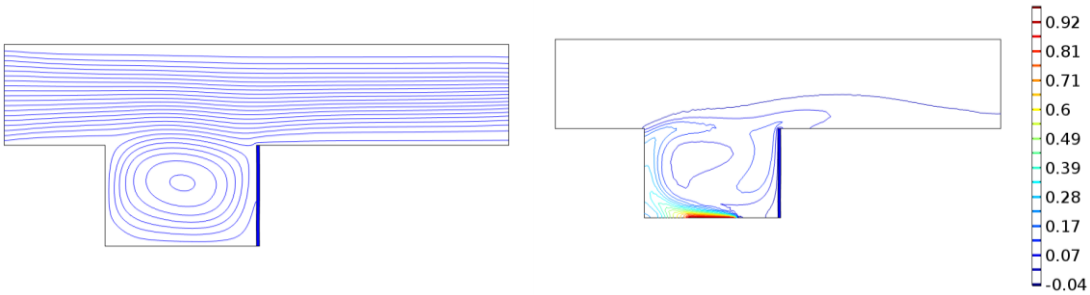

LH = 0.5

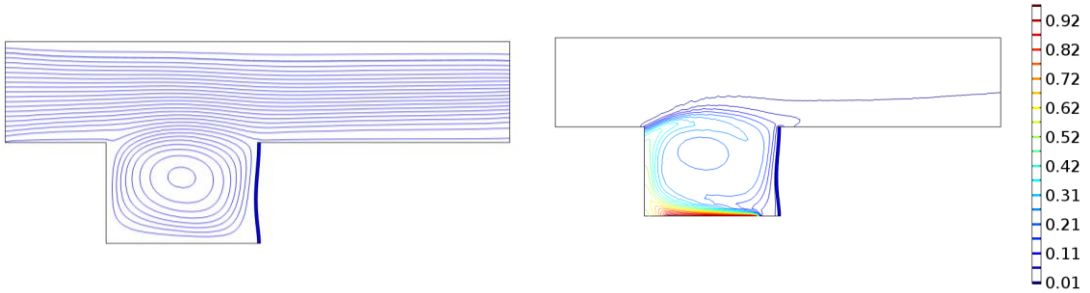

LH = 1

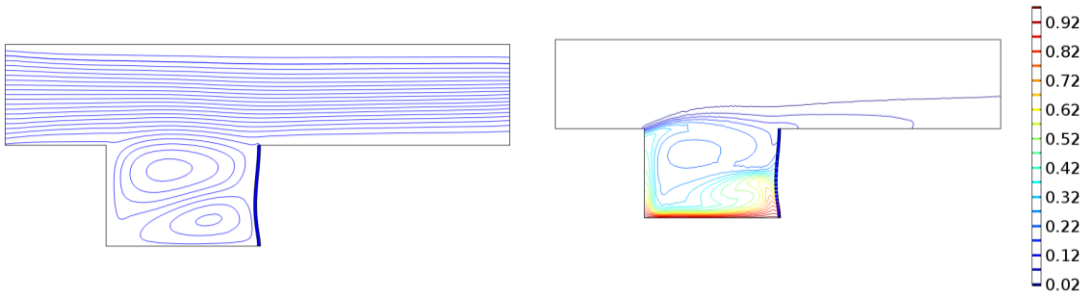

LH = 1.5

Fig. 8: Contour maps for different values of heat source length (LH) when Ca = 10^{-4}, Re = 150, Ri = 10.

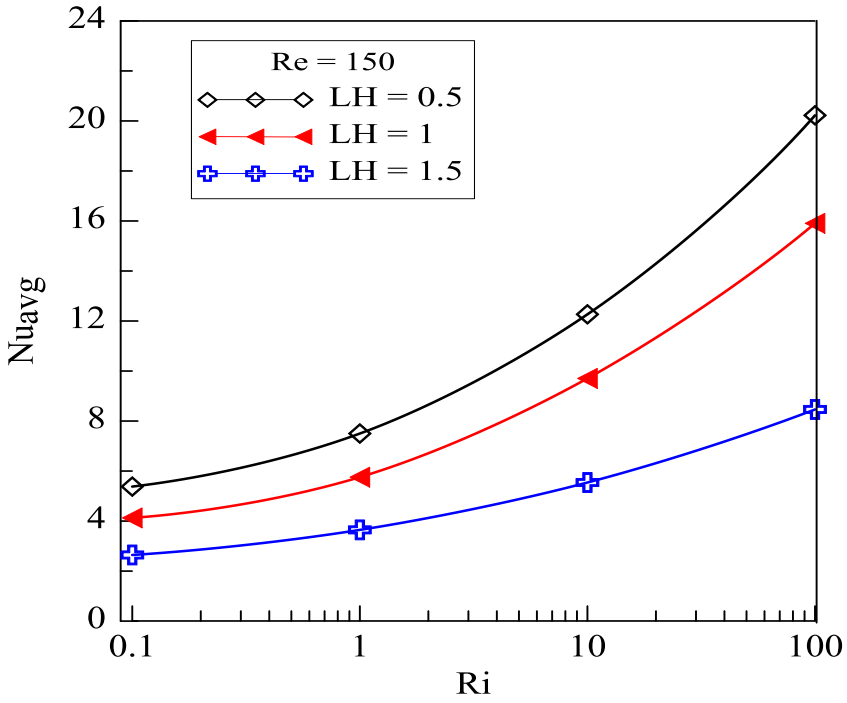

Fig. 9: Variation of Nu_{avg} with the heat source lengthfordifferent Ri values at Re = 150.

Streamlines Isotherms

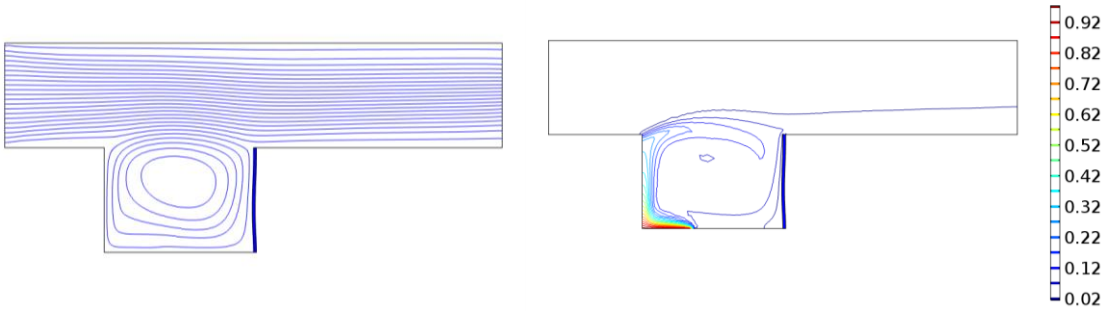

The source is on the left (SL)

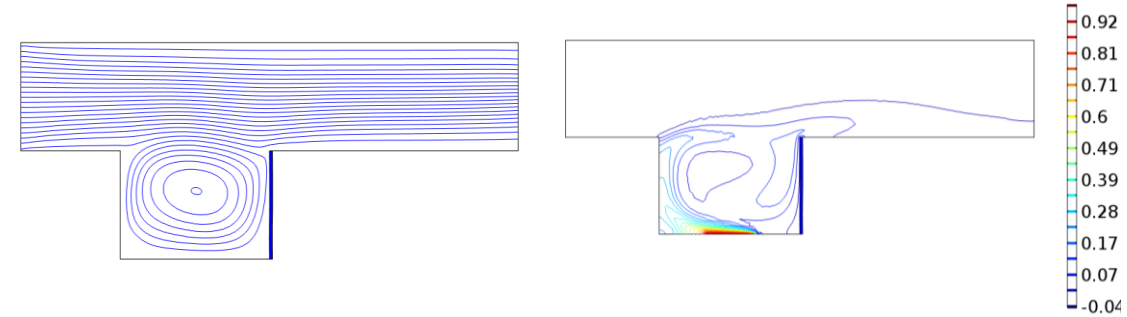

The source is on the middle (SM)

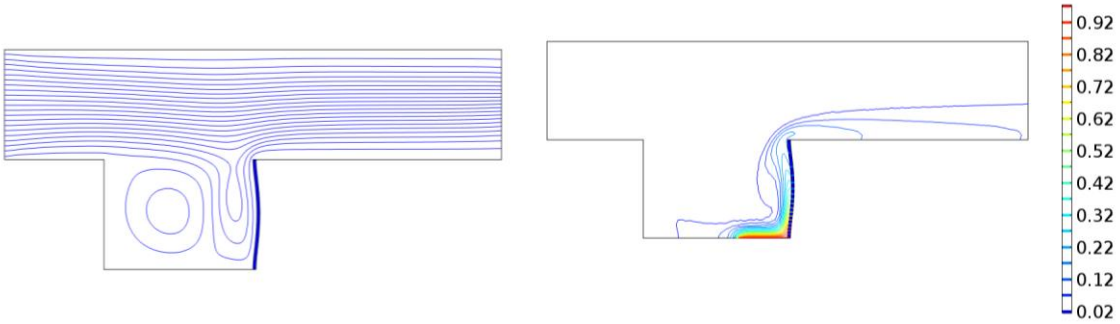

The source is on the right (SR)

Fig. 10: Contour maps for different locations of heat source at Cauchy number Ca = 10^{-4}, (H/D) = 1, Re = 150 and Ri = 10.

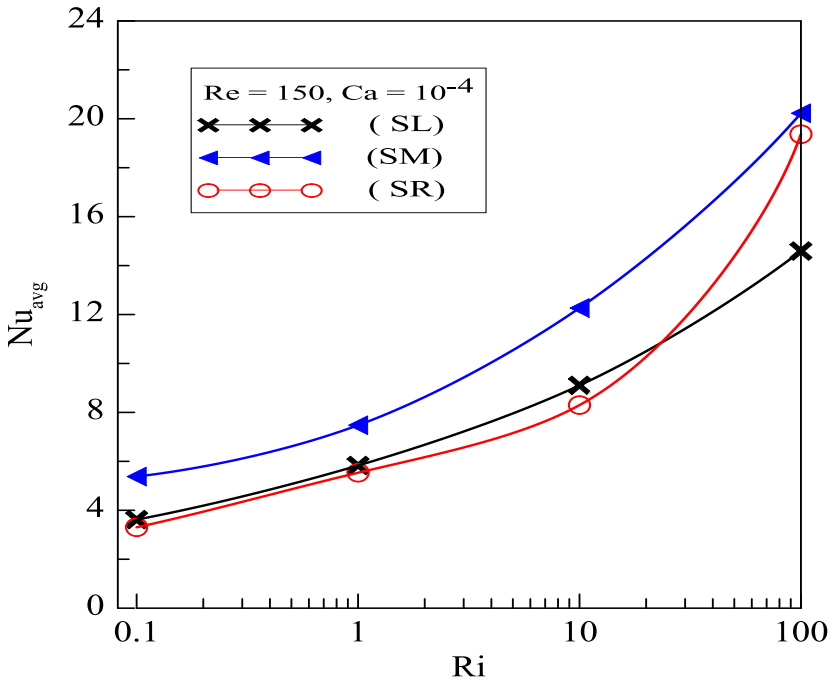

Fig. 11: Variation of the mean Nusselt number with Re for different Ri values at Ca = 10^{-4}